

6. Nishino H, Czurko A, Fukuda A, et al. Pathophysiological process after transient ischemia of the middle cerebral artery in the rat. *Brain Res Bull* 1994;35:51-56.
7. Bowes MP, Rothlein R, Fagan SC, Zivin JA. Monoclonal antibodies preventing leukocyte activation reduce experimental neurologic injury and enhance efficacy of thrombolytic therapy. *Neurology* 1995;45:815-819.
8. Fassbender K, Mössner R, Motsch L, Kischka U, Grau A, Hennerici M. Circulating selectin- and immunoglobulin-type adhesion molecules in acute ischemic stroke. *Stroke* 1995;26:1361-1364.
9. Lefer DJ, Shandelya SML, Serrano CV, Becker LC, Kuppusamy P, Zweier JL. Cardioprotective actions of a monoclonal antibody against CD-18 in myocardial ischemia-reperfusion injury. *Circulation* 1993;88:1779-1787.
10. Wise RJ, Bernardi S, Frackowiak RS, Legg NJ, Jones T. Serial observations on the pathophysiology of acute stroke. The transition from ischaemia to infarction as reflected in regional oxygen extraction. *Brain* 1983;106:197-222.
11. Zhang RL, Chopp M, Li Y, et al. Anti-ICAM-1 antibody reduces ischemic cell damage after transient middle cerebral artery occlusion in the rat. *Neurology* 1994;44:1747-1751.
12. Araki T, Kato H, Inoue T, Kogure K. Long-term observations on calcium accumulation in postischemic gerbil brain. *Acta Neurol Scand* 1991;83:244-249.
13. Dienel GA. Regional accumulation of calcium in postischemic rat brain. *J Neurochem* 1984;43:913-925.
14. Gramsbergen JB, van den Berg KJ. Regional and temporal profiles of calcium accumulation and glial fibrillary acidic protein levels in rat brain after systemic injection of kainic acid. *Brain Res* 1994;667:216-228.
15. Shirohani T, Shima K, Iwata M, Kita H, Chigasaki H. Calcium accumulation following middle cerebral artery occlusion in stroke-prone spontaneously hypertensive rats. *J Cereb Blood Flow Metab* 1994;14:831-836.
16. Siesjo BK, Bengtsson F. Calcium fluxes, calcium antagonists, and calcium-related pathology in brain ischemia, hypoglycemia, and spreading depression: a unifying hypothesis. *J Cereb Blood Flow Metab* 1989;9:127-140.
17. Gramsbergen JBP, Veenma-van der Duin L, Loopuijt L, Paans AMJ, Vaalburg W, Korf J. Imaging of the degeneration of neurons and their processes in rat or cat brain by  $^{45}\text{CaCl}_2$  autoradiography or  $^{55}\text{CoCl}_2$  positron emission tomography. *J Neurochem* 1988;50:1798-1807.
18. Linde R, Laursen H, Hansen AJ. Is calcium accumulation post-injury an indicator of cell damage? *Acta Neurochir* 1995;(suppl):66:15-20.
19. Nagy I, Pabla R, Matesz C, Dray A, Woolf CJ, Urban L. Cobalt uptake enables identification of capsaicin- and bradykinin-sensitive subpopulations of rat dorsal root ganglion cells in vitro. *Neuroscience* 1993;56:241-246.
20. Nilsson P, Laursen H, Hillered L, Hansen AJ. Calcium movements in traumatic brain injury: the role of glutamate receptor-operated ion channels. *J Cereb Blood Flow Metab* 1996;16:262-270.
21. Williams LR, Pregenzer JF, Oostveen JA. Induction of cobalt accumulation by excitatory amino acids within neurons of the hippocampal slice. *Brain Res* 1992;581:181-189.
22. Jansen HML, Pruijm J, Van der Vliet AM, et al. Visualization of damaged brain tissue after ischemic stroke with cobalt-55 positron emission tomography. *J Nucl Med* 1994;35:456-460.
23. Jansen HML, Paans AMJ, Van der Vliet AM, et al. Cobalt-55 positron emission tomography in ischemic stroke. *Clin Neurol Neurosurg* 1997;99:6-10.
24. Jansen HML, Van der Naalt J, Van Zomeren AH, et al. Cobalt-55 positron emission tomography in traumatic brain injury: a pilot study. *J Neurol Neurosurg Psych* 1996;60:221-223.
25. Jansen HML, Knollema S, Veenma-van der Duin L, et al. Pharmacokinetics and dosimetry of 55- and 57-cobalt chloride. *J Nucl Med* 1996;37:2082-2086.
26. Jansen HML, Willemsen ATM, Sinnige LGF, et al. Cobalt-55 positron emission tomography in relapsing-progressive multiple sclerosis. *J Neurol Sci* 1995;132:139-145.
27. Joosten AAJ, Jansen HML, Piers A, Minderhoud JM, Korf J. Cobalt-57 SPECT in relapsing-progressive multiple sclerosis: a pilot study. *Nucl Med Commun* 1995;16:703-705.
28. Orgogozo JM, Dartigues JF. Methodology of clinical trials in acute cerebral ischemia: survival, functional and neurological outcome measures. *Cerebrovasc Dis* 1991;1(suppl 1):100-111.
29. Jacobs A, Put E, Ingels M, Bossuyt A. Prospective evaluation of technetium-99m-HMPAO SPECT in mild and moderate traumatic brain injury. *J Nucl Med* 1994;35:942-947.
30. Dux E, Oschlies U, Uto A, et al. Serum prevents glutamate mitochondrial calcium accumulation in primary neuronal cultures. *Acta Neuropathol* 1996;92:264-272.
31. Furlan M, Marchal G, Vader F, Derlon J-M, Baron J-C. Spontaneous neurological recovery after stroke and the fate of the ischemic penumbra. *Ann Neurol* 1996;40:216-226.
32. Powers WJ, Grubb RL, Darriet D, Raichle ME. Cerebral blood flow and cerebral metabolic rate of oxygen requirements for cerebral function and viability in humans. *J Cereb Blood Flow Metab* 1985;5:600-608.

## Evaluation of Carbon-11-Labeled KF17837: A Potential CNS Adenosine A<sub>2a</sub> Receptor Ligand

Junko Noguchi, Kiichi Ishiwata, Shin-ichi Wakabayashi, Tadashi Nariai, Seigo Shumiya, Shin-ichi Ishii, Hinako Toyama, Kazutoyo Endo, Fumio Suzuki and Michio Senda

Positron Medical Center and Department of Laboratory Animal Science, Tokyo Metropolitan Institute of Gerontology, Tokyo; Showa College of Pharmaceutical Sciences, Tokyo; Department of Neurosurgery, Tokyo Medical and Dental University, Tokyo; and Pharmaceutical Research Laboratories, Kyowa Hakko Kogyo Company, Shizuoka, Japan

The  $^{11}\text{C}$ -labeled KF17837 ([7-methyl- $^{11}\text{C}$ ](E)-8-(3,4-dimethoxy-styryl)-1,3-dipropyl-7-methylxanthine) was evaluated as a PET ligand for mapping adenosine A<sub>2a</sub> receptors in the central nervous system (CNS). **Methods:** The regional brain distribution of [ $^{11}\text{C}$ ]KF17837 and the effect of adenosine antagonists on the distribution were measured in mice by the tissue sampling method. In rats, the regional brain uptake of [ $^{11}\text{C}$ ]KF17837 and the effect of carrier KF17837 was visualized by autoradiography. Imaging of the monkey brain with [ $^{11}\text{C}$ ]KF17837 was performed by PET. **Results:** In mice, a high uptake of [ $^{11}\text{C}$ ]KF17837 was found in the striatum in which A<sub>2a</sub> receptors were highly enriched. The uptake was decreased by co-injection of carrier KF17837 or a xanthine-type A<sub>2a</sub> antagonist CSC but not by nonxanthine-type A<sub>2a</sub> antagonists ZM 241385 or SCH 58261, or an A<sub>1</sub> antagonist KF15372. In the rat brain, [ $^{11}\text{C}$ ]KF17837 was accumulated higher in the striatum than in other brain regions, and the uptake was blocked by co-injection of carrier KF17837. In a monkey PET study, a high striatal uptake of radioactivity was observed. **Conclusion:** Carbon-11-KF17837 binds to

adenosine A<sub>2a</sub> receptors in the striatum. However, the presence of an unknown but specific binding site for xanthine-type compounds also was suggested in the other brain regions. The results also suggested that the in vivo receptor-binding sites of xanthine-type ligands are slightly different from those of nonxanthine-type A<sub>2a</sub> antagonists.

**Key Words:** carbon-11-KF17837; xanthine; adenosine A<sub>2a</sub> receptor; central nervous system; PET

*J Nucl Med* 1998; 39:498-503

Adenosine is an endogenous modulator of synaptic functions in the central nervous system (CNS) as well as in the peripheral system. The effect is mediated by two major subtypes of receptors: adenosine A<sub>1</sub> receptors, which exhibit higher affinity to adenosine and inhibit adenylyl cyclase, and A<sub>2</sub> receptors, which exhibit lower affinity to adenosine and stimulate adenylyl cyclase. Recent advances in molecular biology and pharmacology have demonstrated the presence of at least five subtypes, i.e., A<sub>1</sub>, A<sub>2a</sub>, A<sub>2b</sub>, A<sub>3</sub> and A<sub>4</sub> receptors. They act with guanosine triphosphate-binding proteins and are coupled not only to adenylyl cyclase but also to ion channels and phospholipases.

Received Jan. 3, 1997; revision accepted Jun. 12, 1997.

For correspondence or reprints contact: Kiichi Ishiwata, PhD, Positron Medical Center, Tokyo Metropolitan Institute of Gerontology, 1-1 Naka-cho, Itabashi, Tokyo 173, Japan.

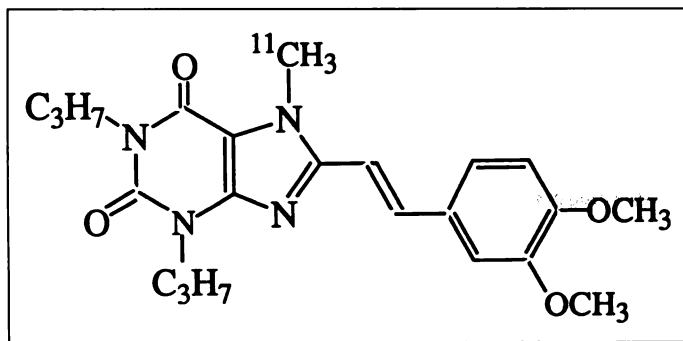


FIGURE 1. Structural formula of [ $^{11}\text{C}$ ]KF17837.

The current status of the adenosine receptors has been reviewed (1–5).

In the CNS,  $A_1$  receptors are present throughout the presynaptic region of excitatory neurons, being rich in the hippocampus, cerebral cortex, thalamic nuclei, basal ganglia and cerebellar cortex in animals (6–9) and humans (10).  $A_{2a}$  receptors are highly enriched in the striatum, nucleus accumbens and olfactory tubercle in which dopamine D1 and D2 receptors also are localized with very high densities (11–13), whereas  $A_{2b}$  receptors show a ubiquitous distribution. By the *in situ* hybridization technique, adenosine  $A_{2a}$  receptor mRNA and dopamine D2-receptor mRNA were found to be mainly expressed in striatopallidal  $\gamma$ -aminobutyric acid (GABA)-enkephaline neurons (14–16). In the patients with Huntington's chorea with a selective degeneration of the striatopallidal neurons, the  $A_{2a}$  receptor density is significantly reduced in the striatum, whereas the density is not affected significantly in the patients with Parkinson's disease characterized by a selective degeneration of nigrostriatal dopamine neurons (17). Recent pharmacological and biochemical data suggest the presence of a receptor-receptor interaction between adenosine  $A_{2a}$  and dopamine D2-receptors in the striatum (18). Adenosine  $A_{2a}$  receptors also mediate striatal GABA and acetylcholine release (19,20).

During the last decade, many neuroreceptors in humans and other animals have been visualized *in vivo* by PET with corresponding radioligands. Although adenosine itself is not a neurotransmitter, PET assessment of the adenosine receptor system offers the opportunity to understand the general neurotransmission system because of its physiological functions of modulating the neuroreceptor system nonspecifically. Recently, we have developed PET ligands for the two adenosine receptor subtypes: [ $^{11}\text{C}$ ]KF15372 ([3-propyl- $^{11}\text{C}$ ]8-dicyclopropylmethyl-1,3-dipropylxanthine) (21,22) and its methyl and ethyl derivatives (23) for adenosine  $A_1$  receptors, and [ $^{11}\text{C}$ ]KF17837 {[7-methyl- $^{11}\text{C}$ ](*E*)-8-(3,4-dimethoxystyryl)-1,3-dipropyl-7-methylxanthine} (Fig. 1) for the adenosine  $A_{2a}$  receptors (24). The selectivity and usefulness of [ $^{11}\text{C}$ ]KF15372 and its derivatives as PET  $A_1$  receptor ligands have been demonstrated in the previous studies (22,23). In a preliminary tissue distribution study of [ $^{11}\text{C}$ ]KF17837, a higher striatal uptake of the tracer was confirmed in rodents (24). *In vitro* autoradiography with [ $^3\text{H}$ ]KF17837 also indicated that the compound is a selective adenosine  $A_{2a}$  ligand (25). In this study, we characterize the properties of [ $^{11}\text{C}$ ]KF17837 *in vivo* as a PET tracer in mice, rats and monkeys.

## MATERIALS AND METHODS

(*E*)-8-(3,4-dimethoxystyryl)-1,3-dipropyl-7-methylxanthine (KF17837) and (*E*)-8-(3,4-dimethoxystyryl)-1,3-dipropylxanthine, 8-(3-chlorostyryl) caffeine (CSC), (4-(2-[7-amino-2-(2-

furyl)[1,2,4]-triazolo[2,3-a][1,3,5]triazin-5-yl-amino]ethyl)phenol) (ZM 241385) 5-amino-7-(2-phenylethyl)-2-(2-furyl)-pyrazolo[4,3-e]-1,2,4-triazolo[1,5-c]pyrimidine (SCH 58261) and 8-dicyclopropylmethyl-1,3-dipropylxanthine (KF15372) were synthesized by Kyowa Hakko Kogyo Company. Alloxazine was obtained from Aldrich Chemical Company, Inc. (Milwaukee, WI) and 1,3-dipropyl-7-methylxanthine (DPMX) was obtained from Research Biochemical, Inc. (Natic, MA).

Radiosynthesis of [ $^{11}\text{C}$ ]KF17837 (Fig. 1) was performed by  $^{11}\text{C}$ -methylation of (*E*)-8-(3,4-dimethoxystyryl)-1,3-dipropylxanthine as described previously (24). The specific activity was 37–64 GBq/ $\mu\text{mol}$ .

## Regional Brain Distribution Study in Mice

We used three groups of male ddY mice (29–38 g). In the first group, [ $^{11}\text{C}$ ]KF17837 (450–550 kBq/9.2–20 pmol) was injected intravenously into mice; and the second group was given [ $^{11}\text{C}$ ]KF17837 (450–550 kBq/9.2–20 pmol) together with carrier KF17837 (50 nmol). These mice were killed at 5, 15, 30 and 60 min after injection by cervical dislocation ( $n = 4$ ). In the third group, [ $^{11}\text{C}$ ]KF17837 (540–1100 kBq/22–91 pmol) was co-injected with one of the following adenosine antagonists into mice. KF17837 (50 nmol,  $K_i$ :  $A_1$ , 62 nM;  $A_{2a}$ , 1.0 nM) (26), CSC (100 nmol,  $K_i$ :  $A_1$ , 28  $\mu\text{M}$ ;  $A_{2a}$ , 54 nM) (27,28) and DPMX (100 nmol,  $K_i$ :  $A_1$ , 7  $\mu\text{M}$ ;  $A_{2a}$ , 1.2  $\mu\text{M}$ ) (29) are xanthine type  $A_2$  antagonists. ZM 241385 (375 nmol,  $K_i$ :  $A_1$ , 510 nM;  $A_{2a}$ , 0.91 nM) (30), SCH 58261 (50 nmol,  $K_i$ :  $A_1$ , 121 nM;  $A_{2a}$ , 2.3 nM) (31) and alloxazine (100 nmol,  $K_i$ :  $A_1$ , 5.25  $\mu\text{M}$ ;  $A_{2a}$ , 2.72  $\mu\text{M}$ ) (11) are nonxanthine  $A_2$  antagonists. KF15372 (100 nmol,  $K_i$ :  $A_1$ , 3.0 nM;  $A_{2a}$ , 430 nM) (32) is a xanthine type  $A_1$  antagonist. The mice were killed 15 min after injection ( $n = 22$  for control and  $n = 4$  for each of the other groups). Blood was collected by heart puncture. The brain was removed and divided into the striatum, cerebellum and cortex. The tissue uptake of radioactivity was expressed as the percent injected dose per gram of tissue (% ID/g).

## Autoradiographic Study in Rats

Male Wistar rats (220–270 g) were killed 15 min after intravenous injection of [ $^{11}\text{C}$ ]KF17837 (67–216 MBq/0.84–13.2 nmol,  $n = 4$ ). The effect of co-injected carrier KF17837 (100 nmol/animal,  $n = 3$ ; and 700 nmol/animal,  $n = 3$ ) on the brain uptake also was measured at 15 min after injection. Coronal and sagittal brain sections were prepared as described previously (22). For the coronal section, the right brain hemisphere of the rat injected with [ $^{11}\text{C}$ ]KF17837 and the left brain hemisphere of the rat given [ $^{11}\text{C}$ ]KF17837 with carrier KF17837 were put side by side to make the hybrid brain for comparative demonstration. Regional brain uptake was analyzed using an imaging plate and a bioimaging analyzer of type BAS 3000 (FUJIX, Fuji Photo Film Co., Tokyo, Japan). The regional brain uptake of radioactivity was measured as the photo-stimulated luminescence (PSL) and expressed as the PSL/ $\text{mm}^2/\text{MBq}$  in which the injected dose was decay-corrected at the contact time.

## PET Study in a Monkey

A female rhesus monkey (22 yr, 3.4 kg) was anesthetized with 0.01–0.05% isoflurane. Carbon-11-KF17837 (97 MBq/2.2 nmol) was injected intravenously into the monkey, and the time sequential tomographic scanning was performed in the coronal section of the brain for 60 min (10 frames for 1 min, 4 frames for 5 min and 3 frames for 10 min). The PET camera used was a model SHR 2000 (Hamamatsu Photonic, Hamamatsu, Japan), which consists of four ring detectors and accommodates seven slices with a resolution of 4.0 mm FWHM in the transaxial plane (33). Regions of interest (ROI) were placed on the striatum, cortex, cerebellum and thalamus, and the time-activity curve in the ROI was obtained for each

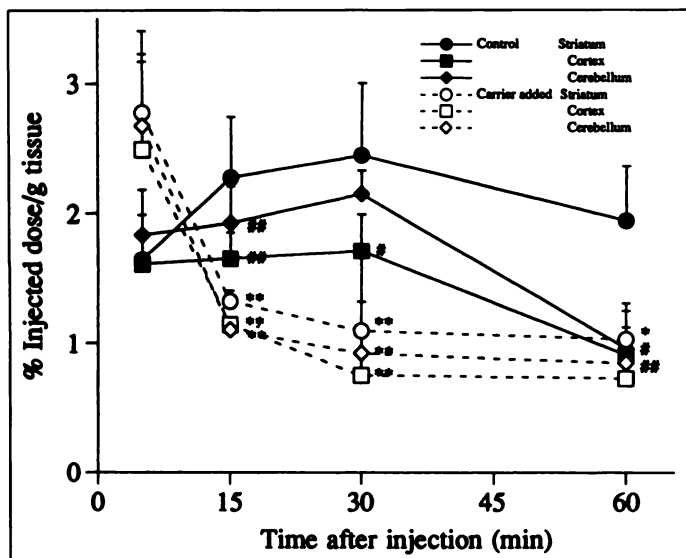


**FIGURE 2.** Regional brain distribution of radioactivity and effect of co-injected carrier KF17837 after an intravenous injection of [<sup>11</sup>C]KF17837 into mice. Injection dose was 450–550 kBq/9.2–20 pmol. Student's t-test was performed between the striatum and cortex or cerebellum in the control, \* represents  $p < 0.1$  and \*\* represents  $p < 0.01$ . Between the control and carrier-loading group, \* represents  $p < 0.1$  and \*\* represents  $p < 0.01$ . Solid and open symbols represent the control and carrier-loading group, respectively. Circle = striatum; square = cortex; and diamond = cerebellum.

scan of the brain as described (34). The radioactivity value was expressed as the standardized uptake value [SUV, (regional activity/milliliter volume)/injected activity/gram body weight].

## RESULTS

### Regional Brain Distribution Study in Mice

Figure 2 shows the regional brain uptake of [<sup>11</sup>C]KF17837 in mice and the effect of co-injected carrier KF17837 on the uptake. In the control, the uptake of [<sup>11</sup>C]KF17837 by the striatum, cortex and cerebellum gradually increased up to 30 min and then decreased. The uptake was much higher in the striatum than in the cortex and cerebellum after 15 min. By co-injection of carrier KF17837, the tracer uptake by the striatum, cortex and cerebellum was enhanced at 5 min after injection but was reduced markedly 15 min after injection in the three regions. At 30 min, the tracer uptake was decreased to the lowest level, one-third of the controls. At 60 min, no difference in the uptake by the cortex and cerebellum was found between

the control and carrier-loading group, although the striatal uptake was significantly reduced by the carrier-loading.

Table 1 shows the effects of co-injection of several adenosine antagonists. The tracer uptake by the striatum, cortex and cerebellum was decreased by carrier KF17837 or a xanthine-type A<sub>2a</sub> antagonist CSC but was not affected by a weak xanthine-type A<sub>2a</sub> antagonist DPMX. The uptake was not affected by nonxanthine-type A<sub>2a</sub> antagonists ZM 241385, SCH 58261 or alloxazine or an A<sub>1</sub> antagonist KF15372.

### Autoradiographic Study in Rats

Figure 3 shows the autoradiographic images of coronal and sagittal brain sections of the rats. In the coronal section (Fig. 3A), [<sup>11</sup>C]KF17837 was accumulated higher in the striatum than in the cortex. In the sagittal section (Fig. 3B), the regional brain distribution was visualized clearly. The mean uptake assessed as the PSL/mm<sup>2</sup>/MBq was 0.89 (n = 4) in the striatum, 0.59 (n = 4) in the cortex and 0.74 (n = 3) in the cerebellum. When carrier KF17837 (700 nmol/animal) was co-injected (Figs. 3A and 3C), the brain structure disappeared, and the mean uptake values were decreased to 0.61 (n = 3) in the striatum, 0.45 (n = 3) in the cortex and 0.51 (n = 2) in the cerebellum. In the control brain, the mean striatum-to-cortex ratio was 1.51 and the mean striatum-to-cerebellum ratio was 1.20. By co-injection of carrier KF17837 (700 nmol), the striatum-to-cortex ratio was 1.36 and the striatum-to-cerebellum ratio was 1.20. When 100 nmol of KF17837 was co-injected, the image was similar to that of the control (data not shown) and the mean striatum-to-cortex ratio was 1.56 (n = 3) and the mean striatum-to-cerebellum ratio was 1.24 (n = 2).

### PET Study in a Monkey

Figure 4 shows images of the rhesus monkey brain acquired by PET with [<sup>11</sup>C]KF17837. A high uptake of radioactivity was observed in the striatum. The uptake also was visualized in the cortex, cerebellum and thalamus. The time-activity curves in these regions during 60 min are shown in Figure 5. The radioactivity level (SUV) in the striatum was slightly higher than those in other brain regions. The striatal activity level was retained for the initial 20 min and then gradually decreased with time. The uptake ratio of striatum-to-cortex, striatum-to-cerebellum and striatum-to-thalamus was 1.38, 1.32 and 1.38, respectively, 30 min after injection.

**TABLE 1**

Effect of Adenosine Antagonists on the Regional Brain Distribution of Radioactivity at 15 Minutes After Intravenous Injection of Carbon-11-KF17837 into Mice

Antagonist (nmol)*	Percent injection dose/gram tissue			
	Blood	Striatum	Cortex	Cerebellum
Control	0.84 ± 0.13	2.28 ± 0.47	1.65 ± 0.20	1.93 ± 0.28
KF17837 (50)	1.19 ± 0.05	1.32 ± 0.09 <sup>‡</sup>	1.14 ± 0.02 <sup>†</sup>	1.10 ± 0.03 <sup>‡</sup>
CSC (100)	1.16 ± 0.18	2.02 ± 0.51	1.27 ± 0.26 <sup>†</sup>	1.38 ± 0.29 <sup>†</sup>
DPMX (100)	0.97 ± 0.21	2.33 ± 0.41	1.93 ± 0.24	2.20 ± 0.26
ZM 241385 (375)	0.96 ± 0.10	2.60 ± 0.05	2.08 ± 0.10	2.37 ± 0.22
SCH 58261 (50)	1.07 ± 0.08	2.75 ± 0.24	2.45 ± 0.39	2.77 ± 0.55
Alloxazine (100)	0.80 ± 0.13	1.96 ± 0.39	1.74 ± 0.42	1.96 ± 0.50
KF15372 (100)	1.06 ± 0.09	2.31 ± 0.37	1.83 ± 0.17	2.07 ± 0.32

\*Co-injected doses of antagonists are indicated in parentheses.

Student's t-test was performed between the control and the group given antagonists:

<sup>†</sup> $p < 0.01$  and <sup>‡</sup> $p < 0.001$ .

Mean ± s.d. (control, n = 22 and other groups, n = 4). Injection dose: 540–1100 MBq/22–91 pmol.

## DISCUSSION

In this study, we have characterized the *in vivo* properties of [ $^{11}\text{C}$ ]KF17837 as a PET tracer. In mice, rats and a monkey, the tracer was taken up at a higher level by the striatum, which is rich in the adenosine  $A_{2a}$  receptors, than by the other brain regions. This is consistent with the distribution of adenosine  $A_{2a}$  receptors demonstrated by an *in vitro* binding assay with the brain membrane fraction (11) or by autoradiography (ARG) (12,13) and with that of  $A_{2a}$  receptor mRNA measured by the *in situ* hybridization technique (14–16).

In the competition study, the tracer uptake was enhanced in 5 min by carrier loading in the striatum, cortex and cerebellum. This phenomenon may be derived from the altered peripheral absorption or pharmacological effect of a large amount of KF17837. On the other hand, after 5 min the striatal uptake of the tracer was significantly decreased. While the uptake in the cortex and cerebellum was also clearly blocked at 15 and 30 min, the tracer was washed out from the cortex and cerebellum but not from the striatum at 60 min, leaving the binding of the tracer in the cortex and cerebellum at a nonspecific level. The binding of the tracer in the striatum and in the cortex and cerebellum may have differing kinetics. The slight reduction also was observed by co-injection of a xanthine type  $A_{2a}$  antagonist CSC, though the difference was not significant in case of the striatum, but not by co-injection of a weak  $A_{2a}$  antagonist DPMX or a strong  $A_1$  antagonist KF15372. These findings suggested that [ $^{11}\text{C}$ ]KF17837 has a selective affinity for adenosine  $A_{2a}$  receptors.

In the regional brain distribution study, the tracer uptake by the cortex and cerebellum, which lack  $A_{2a}$  receptors, also was decreased by co-injection of KF17837 or CSC. The phenomenon also was detected in the present *ex vivo* and a previous *in vitro* ARG studies (25). In the *in vitro* ARG study on [ $^3\text{H}$ ]KF17837S, in which an active *E*-form (18%) of [ $^3\text{H}$ ]KF17837 and an inactive *Z*-isomer (82%) were mixed, the specific binding *in vitro* was 26% of the total binding in the cerebral cortex and 12% in the cerebellum (25). The corresponding figures assessed by the blocking effect on the *ex vivo* ARG were 24% in the cortex and 31% in the cerebellum. These findings suggest the presence of unknown but specific binding sites for xanthine-type compounds in the cortex and cerebellum, considering both the differing kinetics of the tracer binding in the cortex and cerebellum and in the striatum as described

above. A possibility is that KF17837 may have an affinity for  $A_{2b}$  receptor *in vivo* as well. We tried alloxazine as a weak  $A_{2b}$  antagonist (35) because a selective adenosine  $A_{2b}$  antagonist was not available, but it did not reduce the uptake of [ $^{11}\text{C}$ ]KF17837. However, we cannot determine whether the [ $^{11}\text{C}$ ]KF17837 binds to the  $A_{2b}$  receptors or not.

The *in vitro* ARG has shown that the total [ $^3\text{H}$ ]KF17837S-binding was concentrated 2.3–3.0 times higher in the striatum than in the other regions (25). The specific binding assessed by competition with a large amount of carrier KF17837S was 64% in the striatum. When the cortex and cerebellum were assumed to be the reference region free of  $A_{2a}$  receptors, the specific binding (striatum minus reference region) was estimated to be 56–67% from their data. On the other hand, the present *ex vivo* ARG study has shown that the total [ $^{11}\text{C}$ ]KF17837 uptake was 1.2–1.5 times higher in the striatum than in the other regions at 15 min postinjection (Fig. 3B). The  $A_{2a}$  receptors-specific uptake by the striatum was 31% of the total uptake assessed by the self-competition or 17–34% assessed by the difference between the striatum and reference regions. The investigated time may not be an ideal point for comparing *in vitro* and *in vivo* data. We performed the blocking studies in the regional brain distribution in mice and in the ARG in rats at 15 min after tracer injection because of the short-half life of  $^{11}\text{C}$ . In mice, the specific uptake assessed by the self-competition at this time was approximately two-thirds that of the highest specific uptake at 30 min postinjection. Because of the susceptibility of a xanthine compound to metabolic alterations (22,23), the labeled metabolites possibly affect the assessment of the specific binding of the tracer *in vivo*.

The co-injection of nonxanthine-type adenosine antagonists ZM 241385 or SCH 58261, which have a high affinity for the  $A_{2a}$  receptors, did not reduce the uptake of [ $^{11}\text{C}$ ]KF17837, although the affinity of ZM 241385 (30) and SCH 58261 (31) for the  $A_{2a}$  receptors is 180 times and 20 times, respectively, higher than that of xanthine-type CSC (27,28) in the membrane binding assay. One possibility is that a sufficient amount of ZM 241385 or SCH 58261 to block the receptor binding of the tracer did not enter the brain. However, both compounds are lipophilic. Therefore, it is doubtful that both compounds would have had difficulty crossing the blood-brain barrier. On the other hand, if all the ZM 241385 and SCH 58261 penetrated the blood-brain barrier, the blocking effect of both compounds on the different regions of the brain would still be less than CSC based on our finding that [ $^{11}\text{C}$ ]KF17837 also has an affinity for the myocardial adenosine  $A_{2a}$  receptors (24). The blocking effect of ZM 241385 and SCH 58261 on the myocardial uptake of [ $^{11}\text{C}$ ]KF17837 was smaller than that of CSC (data will be described elsewhere). There is no barrier in the heart that corresponds to the blood-brain barrier in the CNS. Therefore, the most logical explanation would be that xanthine-type and nonxanthine-type antagonists may recognize different binding sites besides the common binding site within the  $A_{2a}$  receptor *in vivo*. Alternatively, the *in vivo* configuration of the receptor molecule itself or of the receptor-containing region of the plasma membrane may provide different binding sites for the xanthine-type and nonxanthine-type structures.

This study demonstrated the adenosine  $A_{2a}$  receptors in the primate brain *in vivo* by PET. By the PET scanning, the striatal uptake of [ $^{11}\text{C}$ ]KF17837 was visualized clearly, and the SUV value was larger in the striatum than in the cortex, cerebellum and thalamus of the monkey. When the uptake in reference brain regions besides the striatum was assumed to be the nonspecific binding, the  $A_{2a}$  receptor-specific binding of the

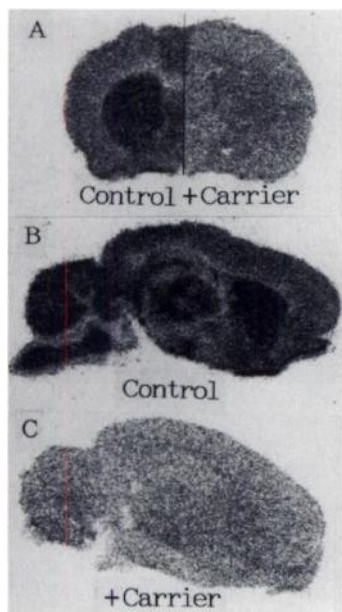


**FIGURE 3.** Autoradiograms of the brain section at 15 min after an intravenous injection of [ $^{11}\text{C}$ ]KF17837 with and without carrier KF17837 into rats. (A) Coronal section of rat brain in which the right hemisphere of the control and the left hemisphere of the rat given carrier-loading [ $^{11}\text{C}$ ]KF17837 were put side-by-side for comparison. The left side shows a control image and the right side shows a carrier-added image. (B) Control sagittal section. (C) Carrier-added sagittal section.

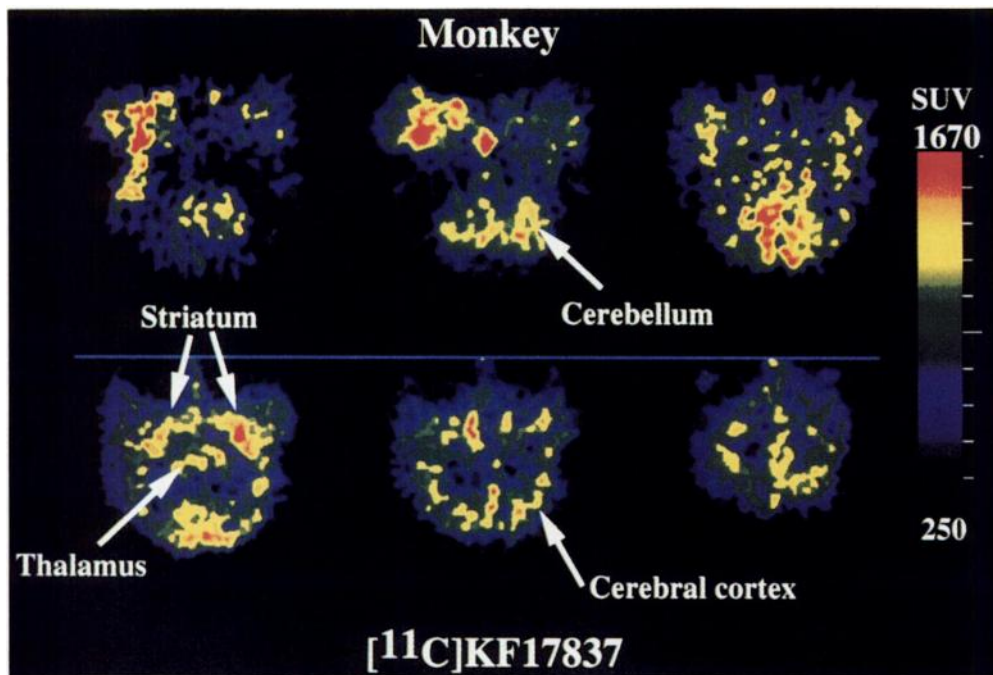


**FIGURE 4.** PET images of the anesthetized monkey brain with [ $^{11}\text{C}$ ]KF17837. The images were acquired for 50 min starting at 10 min after the injection. Injection dose was 97 MBq/2.2 nmol. The values in the color scale are SUV by  $10^4$  times.

[ $^{11}\text{C}$ ]KF17837 was approximately 28% of the total striatal uptake.

#### CONCLUSION

The regional brain distribution and blocking studies in mice, ex vivo ARG with blocking studies in rats and PET imaging in primates have suggested that [ $^{11}\text{C}$ ]KF17837 binds adenosine  $A_{2a}$  receptors in the striatum. However, the presence of an unknown but specific binding site for the xanthine-type compounds also was suggested in the other brain regions.

#### ACKNOWLEDGMENTS

We thank Dr. S. Shibabe for his advice and discussion on the ARG studies, and the Radioisotope School Nuclear Education Center, Japan Atomic Energy Research Institute (Tokyo, Japan), where the ARG was analyzed. We thank Satoshi Maekawa for his assistance in radiosynthesis and Keiichi Oda, Yojiro Sakiyama and Miyoko Ando for their assistance in the PET study. This work was supported by Grants-in-Aid for Scientific Research (C) No. 07807068 and (A) No. 08557045 from the Ministry of Education, Science, Sports and Culture, Japan.

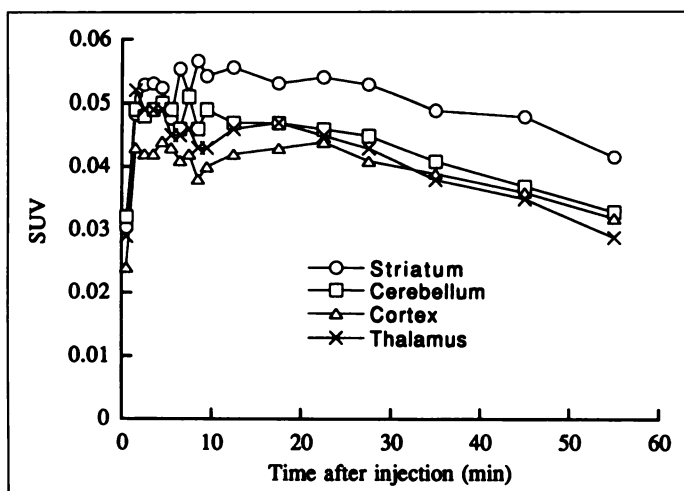


**FIGURE 5.** Time-activity curves in the rhesus monkey brain [ $^{11}\text{C}$ ]KF17837.

#### ADDENDUM

During discussion of the manuscript, Stone-Elander et al. reported the PET study of the same compound in the rhesus monkeys (*Nucl Med Biol* 1997;24:187–191). They stated the limited usefulness of the tracer because of low penetration across the blood-brain barrier and the high nonspecific binding.

#### REFERENCES

- Liang BT. Adenosine receptors and cardiovascular function. *Trends Cardiovasc Med* 1992;2:100–108.
- Jacobson KA, Gallo-Rodriguez C, Melman N, et al. Structure-activity relationships of 8-styrylxanthines as  $A_2$ -selective adenosine antagonists. *J Med Chem* 1993;36:1330–1342.
- Tucker AL, Linden J. Cloned receptors and cardiovascular responses to adenosine. *Cardiovasc Res* 1993;27:62–67.
- Fink JS, Weaver DR, Rivkees SA, et al. Molecular cloning of the rat adenosine receptor: selective co-expression with  $D_2$  dopamine receptors in rat striatum. *Mol Brain Res* 1992;14:186–195.
- Fredholm BB, Abbracchio MP, Burnstock G, et al. Nomenclature and classification of purinoceptors. *Pharmacol Rev* 1994;46:143–156.
- Lewis ME, Patel J, Moon Edley S, Marangos PJ. Autoradiographic visualization of rat brain adenosine receptors using  $N^6$ -cyclohexyl[ $^3\text{H}$ ]adenosine. *Eur J Pharmacol* 1981;73:109–110.
- Goodman RR, Snyder SH. Autoradiographic localization of adenosine receptors in rat brain using [ $^3\text{H}$ ]cyclohexyladenosine. *J Neurosci* 1982;2:1230–1241.
- Pagonopoulou O, Angelatou F, Kostopoulos G. Effect of pentylentetrazol-induced seizures on  $A_1$  adenosine receptor regional density in the mouse brain: a quantitative autoradiographic study. *Neuroscience* 1993;56:711–716.
- Fastbom J, Pazos A, Palacios JM. The distribution of adenosine  $A_1$  receptors and 5'-nucleotidase in the brain of some commonly used experimental animals. *Neuroscience* 1987;22:813–826.
- Fastbom J, Pazos A, Probst A, Palacios JM. Adenosine  $A_1$  receptors in the human brain: a quantitative autoradiographic study. *Neuroscience* 1987;22:827–839.
- Bruns RF, Lu GH, Pugsley TA. Characterization of  $A_2$  adenosine receptor labeled with [ $^3\text{H}$ ]NECA in rat striatal membranes. *Mol Pharmacol* 1986;29:331–346.
- Jarvis MF, Williams M. Direct autoradiographic localization of adenosine  $A_2$  receptors in the rat brain using the  $A_2$ -selective agonist, [ $^3\text{H}$ ]CGS 21680. *Eur J Pharmacol* 1989;168:243–246.
- Parkinson FE, Fredholm BB. Autoradiographic evidence for G-protein coupled  $A_2$ -receptors in rat neostriatum using [ $^3\text{H}$ ]CGS21680 as a ligand. *Naunyn Schmiedebergs Arch Pharmacol* 1990;342:85–89.
- Schiffmann SN, Jacobs O, Vanderhaeghen JJ. Striatal restricted adenosine  $A_2$  receptor (RDC8) is expressed by enkephaline but not substance P neurons: an in situ hybridization histochemistry study. *J Neurochem* 1991;57:1062–1067.
- Schiffmann SN, Libert F, Vassart G, Vanderhaeghen J-J. Distribution of adenosine  $A_2$  receptor mRNA in the human brain. *Neurosci Lett* 1991;130:177–181.
- Pollack AE, Harrison MB, Wooten GF, Fink JS. Differential localization of  $A_{2a}$  adenosine receptor mRNA with  $D_1$  and  $D_2$  dopamine receptor mRNA in striatal output pathways following a selective lesion of striatonigral neurons. *Brain Res* 1993;631:161–166.
- Martinez-Mir MI, Probst A, Palacios JM. Adenosine  $A_2$  receptors: selective localization in the human basal ganglia and alterations with disease. *Neuroscience* 1991;42:697–706.

18. Ferré S, Fuxe K, von Euler G, Johansson B, Fredholm BB. Adenosine-dopamine interactions in the brain. *Neuroscience* 1992;51:501-512.
19. Kirk IP, Richardson PJ. Adenosine A<sub>2a</sub> receptor-mediated modulation of striatal [<sup>3</sup>H]GABA and [<sup>3</sup>H]acetylcholine release. *J Neurochem* 1994;62:960-966.
20. Kurokawa M, Koga K, Kase H, Nakamura J, Kuwana Y. Adenosine A<sub>2a</sub> receptor-mediated modulation of striatal acetylcholine release in vivo. *J Neurochem* 1996;66:1882-1888.
21. Ishiwata K, Furuta R, Shimada J, et al. Synthesis and preliminary evaluation of [<sup>11</sup>C]KF15372, a selective adenosine A<sub>1</sub> antagonist. *Appl Radiat Isot* 1995;46:1009-1013.
22. Furuta R, Ishiwata K, Kiyosawa M, et al. Carbon-11-labeled KF15372: a potential central nervous system adenosine A<sub>1</sub> receptor ligand. *J Nucl Med* 1996;37:1203-1207.
23. Noguchi J, Ishiwata K, Riko Furuta R, et al. Evaluation of carbon-11-labeled KF15372 and its ethyl and methyl derivatives as a potential CNS adenosine A<sub>1</sub> receptor ligand. *Nucl Med Biol* 1997;24:53-59.
24. Ishiwata K, Noguchi N, Toyama H, et al. Synthesis and preliminary evaluation of [<sup>11</sup>C]KF17837, a selective adenosine A<sub>2A</sub> antagonist. *Appl Radiat Isot* 1996;47:507-511.
25. Nonaka H, Mori A, Ichimura M, et al. Binding of [<sup>3</sup>H]KF17837S, a selective adenosine A<sub>2</sub> receptor antagonist, to rat brain membranes. *Mol Pharmacol* 1994;46:817-822.
26. Nonaka Y, Shimada J, Nonaka H, et al. Photoisomerization of a potent and selective adenosine A<sub>2</sub> antagonist, (*E*)-1,3-dipropyl-8-(3,4-dimethoxystyryl)-7-methylxanthine. *J Med Chem* 1993;36:3731-3733.
27. Jacobson KA, Nikodijevic O, Padgett WL, Gallo-Rodriguez C, Maillard M, Daly JW. 8-(3-Chlorostyryl)caffeine (CSC) is a selective A<sub>2</sub>-adenosine antagonist in vitro and in vivo. *FEBS Lett* 1993;323:141-144.
28. Jacobson KA, Gallo-Rodriguez C, Melman N, et al. Structure-activity relationships of 8-styrylxanthines as A<sub>2</sub>-selective adenosine antagonists. *J Med Chem* 1993;36:1333-1342.
29. Daly JW, Padgett WL, Shamim MT. Analogues of caffeine and theophylline: effect of structural alterations on affinity at adenosine receptors. *J Med Chem* 1986;29:1305-1308.
30. Poucher SM, Keddie JR, Singh P, et al. The in vitro pharmacology of ZM 241385, a potent, non-xanthine, A<sub>2a</sub> selective adenosine receptor antagonist. *Br J Pharmacol* 1995;115:1096-1102.
31. Zocchi C, Ongini E, Conti A, et al. The non-xanthine heterocyclic compound SCH 58261 is a new potent and selective A<sub>2a</sub> adenosine receptor antagonist. *J Pharmacol Exp Ther* 1996;276:398-404.
32. Shimada J, Suzuki F, Nonaka H, Ishii A. 8-Polycycloalkyl-1,3-dispropylxanthines as potent and selective antagonists for A<sub>1</sub>-adenosine receptors. *J Med Chem* 1992;35:924-930.
33. Watanabe M, Uchida H, Okada H, et al. A high resolution PET for animal studies. *IEEE Trans Med Imag* 1992;11:577-580.
34. Sakiyama Y, Ishiwata K, Ishii K, et al. Evaluation of the brain uptake properties of [<sup>11</sup>C]labeled hexanoate in anesthetized cats by mean of positron emission tomography. *Ann Nucl Med* 1996;10:361-366.
35. Liang BT, Haltiwanger B. Adenosine A<sub>2a</sub> and A<sub>2b</sub> receptors in cultured fetal chick heart cells. High- and low-affinity coupling to stimulation of myocyte contractility and cAMP accumulation. *Circ Res* 1995;76:242-251.

# Fully Automated Establishment of Stereotaxic Image Orientation in Six Degrees of Freedom for Technetium-99m-ECD Brain SPECT

Jeffrey Tsao, Audrius Stundzia and Masanori Ichise

Department of Nuclear Medicine, Mount Sinai Hospital, and University of Toronto, Toronto, Ontario, Canada

Anatomical localization requires establishing an anatomical space within the image matrix. We developed a fast, fully automated method to establish the image orientation for <sup>99m</sup>Tc-ethylcysteinate dimer (ECD) brain SPECT images. **Methods:** The image orientation of ECD brain SPECT images was established in four stages. First, the brain surface was edge-detected as an isosurface at an adaptive threshold. Second, a "convex hull" was determined for the isosurface to minimize regional variability in brain shape. A principal axis transformation and a symmetry vector analysis were applied to the convex hull to resolve the craniocaudal direction and to estimate the midsagittal plane. Third, the brain orientation was refined from this estimate by location of the interhemispheric fissure, the tentorial groove and the frontotemporal groove on the isosurface. Last, the intercommissural (anterior commissure-posterior commissure, or AC-PC) line was detected on the midsagittal slice, and the Talairach grid was scaled to fit the maximal brain dimensions from the AC-PC line. **Results:** The average absolute errors were 2.3° ± 1.5° and 1.08 mm ± 1.11 mm for the midsagittal plane (n = 24) and 2.04° ± 0.80°, 2.0% ± 1.8% of the brain length and 2.3% ± 2.2% of the brain height for the AC-PC line (n = 8). In addition, this program successfully established the image orientation in 94 of 100 clinical ECD brain SPECT studies. Processing time was <40 sec for 128 × 128 × 50 matrices on a DEC Alpha workstation. **Conclusion:** We have developed a fast, robust and fully automated method that determines the orientation of ECD brain SPECT images. This objective method of standardizing the image orientation should be useful for anatomical localization and clinical interpretation of these images.

**Key Words:** technetium-99m-ECD; brain SPECT; image orientation; automation; image processing

**J Nucl Med** 1998; 39:503-508

In recent years, there has been increasing recognition of the clinical application of functional brain imaging using SPECT and PET. In interpreting these images, it is often essential to accurately localize detected functional signals in the anatomical space of the brain. This anatomical localization requires establishing an anatomical space within the image matrix. The spatial relationship between the anatomical space and the image matrix is referred to as the image orientation, and it is defined by six degrees of freedom (three translational coordinates along and three rotational angles around the x-, y- and z-axes). A common approach to anatomical localization has been the concurrent use of morphological imaging such as MRI or x-ray CT, which provides detailed anatomical information that functional images may lack (1-4). Image coregistration between the two types of imaging modalities allows the image orientation of SPECT or PET to be established in the anatomical space of MRI or CT.

Alternatively, anatomical localization can be achieved by establishing a standard anatomical space, such as the Talairach stereotaxic coordinate system (5), in the functional image. An advantage of this approach is that MRI or CT is not required. Furthermore, this approach enables intersubject comparison of corresponding functional signals by matching signals associated with the same stereotaxic locations. In several reports (6-8), a standard anatomical space has been established by using fiducial markers for the canthomeatal or orbitomeatal lines to estimate the stereotaxic baseline that passes through the anterior and posterior commissures of the brain (the AC-PC line). However, the limitation of this and other fiducial marker-based methods is the significant variability between the external and the true brain orientations (9). An alternative method is to derive information about image orientation, such as the AC-PC line, retrospectively from internal landmarks within the functional image (10-12).

Received Dec. 6, 1996; revision accepted Apr. 23, 1997.

For correspondence or reprints contact: Masanori Ichise, MD, FRCPC(C), Nuclear Medicine, Room 635, Department of Medical Imaging, Mount Sinai Hospital, 600 University Avenue, Toronto, Ontario, Canada M5G 1X5.